

# Stop Treating Collisions Equally: Qualification-Aware Semantic ID Learning for Recommendation at Industrial Scale

Zheng Hu<sup>†</sup>  
University of Electronic  
Science and Technology of  
China  
Chengdu, China

Yuxin Chen\*  
Kuaishou Technology  
Beijing, China  
chenyuxin06@kuaishou.com

Yongsen Pan<sup>†</sup>  
University of Electronic  
Science and Technology of  
China  
Chengdu, China

Xu Yuan  
Yuting Yin  
Daoyuan Wang  
Kuaishou Technology  
Beijing, China

Boyang Xia  
Zefei Luo  
Kuaishou Technology  
Beijing, China

Hongyang Wang  
Songhao Ni  
Kuaishou Technology  
Beijing, China

Dongxu Liang  
Kuaishou Technology  
Beijing, China

Jun Wang  
Kuaishou Technology  
Beijing, China

Shimin Cai  
University of Electronic  
Science and Technology of  
China  
Chengdu, China

Tao Zhou  
University of Electronic  
Science and Technology of  
China  
Chengdu, China

Fuji Ren\*  
University of Electronic  
Science and Technology of  
China  
Chengdu, China  
renfuji@uestc.edu.cn

Wenwu Ou  
Kuaishou Technology  
Beijing, China

## Abstract

Semantic IDs (SIDs) are compact discrete representations derived from multimodal item features, serving as a unified abstraction for ID-based and generative recommendation. However, learning high-quality SIDs remains challenging due to two issues. (1) **Collision problem**: the quantized token space is prone to collisions, in which semantically distinct items are assigned identical or overly similar SID compositions, resulting in semantic entanglement. (2) **Collision-signal heterogeneity**: collisions are not uniformly harmful. Some reflect genuine conflicts between semantically unrelated items, while others stem from benign redundancy or systematic data effects. To address these challenges, we propose **Qualification-Aware Semantic ID Learning (QuaSID)**, an end-to-end framework that learns collision-qualified SIDs by selectively repelling qualified conflict pairs and scaling the repulsion strength by collision severity. QuaSID consists of two mechanisms: Hamming-guided Margin Repulsion, which translates low-Hamming SID overlaps into explicit, severity-scaled geometric constraints on the encoder space; and Conflict-Aware Valid Pair Masking, which masks protocol-induced benign overlaps to de-noise repulsion supervision. In addition, QuaSID incorporates a dual-tower contrastive objective to inject collaborative signals into tokenization. Experiments on public benchmarks and industrial data validate QuaSID. On public datasets, QuaSID consistently outperforms strong baselines, improving top-K ranking quality by **5.9%** over the best baseline while increasing SID composition diversity. In an online A/B test on Kuaishou e-commerce with a 5% traffic split, QuaSID increases ranking GMV-S2 by **2.38%** and improves completed orders on cold-start retrieval by up to **6.42%**. Finally,

we show that the proposed repulsion loss is plug-and-play and enhances a range of SID learning frameworks across datasets.

## CCS Concepts

• Information systems → Recommender systems.

## Keywords

Recommendation systems; semantic IDs; vector quantization; generative recommendation

## 1 Introduction

In modern recommendation systems, Semantic IDs (SIDs) have emerged as a promising mechanism for representing items using compact, discrete codes distilled from rich multimodal features such as text, images, audio, and structured metadata [1, 10, 17, 33]. SIDs can enhance both traditional recommendation pipelines and emerging generative recommendation systems [12, 15]. Unlike conventional ID embeddings that depend on ever-growing embedding tables and ad-hoc hashing, SID-based recommendation represents each item as a fixed-length sequence of discrete semantic tokens [23]. This yields compact, reusable, and index-friendly identifiers that mitigate vocabulary explosion in both retrieval and generation, while reducing hash-induced collision noise and stabilizing item identities under frequent item updates, re-indexing, and real-world life-cycle drift [34]. These properties make SIDs particularly valuable in large-scale industrial environments, where efficiency, interpretability, and cross-system consistency are essential. Moreover, as the field shifts from classical retrieval-and-ranking architectures toward generative recommendation systems (GRS), the importance of SIDs continues to grow [35, 36]. By providing a unified tokenized

\*Corresponding authors.

<sup>†</sup>Work done during internship at Kuaishou Technology.

interface, SIDs allow items to be seamlessly incorporated into generative models, enabling them to generate recommendations in the same manner as they generate language.

Recent progress in discrete representation learning has established Residual Quantized Variational Autoencoders (RQ-VAE) [14] as the mainstream paradigm for mapping multimodal item features into SIDs. By hierarchically quantizing continuous representations into multiple codebooks, RQ-VAE-based methods achieve a favorable balance between expressiveness and compactness, and have demonstrated strong performance across a range of recommendation and generation tasks [16, 30, 33]. Despite their success, existing SID learning frameworks still exhibit two key limitations that restrict their practical effectiveness [15]. Figure 1 summarizes the SID pipeline and the two challenges discussed above. First, SID learning suffers from a severe **collision problem in the discrete space**. When a large corpus of items is compressed into quantized codes, RQ-VAE models often exhibit uneven codebook utilization or centroid collapse during training, causing many semantically unrelated items to be mapped to identical or highly similar SID compositions. Such unintended collisions lead to semantic entanglement, making it difficult for downstream models to distinguish conceptually distinct items. Second, **collision signals observed during training are highly heterogeneous and require finer-grained qualification**. Apparent SID collisions (i.e., identical or highly overlapping code compositions) may reflect genuinely harmful conflicts between unrelated items, but they can also arise from benign factors such as repeated sampling of the same item or task-consistent relations intentionally introduced by the training pipeline. Without differentiating these cases, a one-size-fits-all collision suppression strategy may inadvertently push apart benign pairs and interfere with downstream alignment.

To address these challenges, we propose **Qualification-Aware Semantic ID Learning (QuaSID)**, an end-to-end SID learning framework that learns collision-qualified SIDs by applying repulsion only to qualified conflict pairs and calibrating the repulsion strength by collision severity. QuaSID introduces Hamming-guided Margin Repulsion (HaMR), which converts unexpectedly low Hamming distances between SIDs observed during training into explicit geometric margin constraints on the encoder space. When semantically unrelated items exhibit overly small Hamming distances in their SID compositions, HaMR interprets such cases as insufficient separation in the learned representations and enforces adaptive separation in the continuous embedding space, with penalty strength modulated by collision severity. To avoid repulsing benign overlaps or structurally biased pairs, QuaSID further employs Conflict-Aware Valid Pair Masking (CVPM), which excludes same-item duplicates and constructed collaborative positives from collision supervision, yielding a cleaner supervision set for repulsion-based learning. Finally, QuaSID integrates a dual-tower contrastive objective to inject collaborative signals into the tokenization process, which helps align SIDs with downstream recommendation objectives. We conduct extensive offline and online experiments to validate QuaSID. On public benchmarks, QuaSID improves top- $K$  ranking quality by **5.9%** on average over the best baseline while also increasing SID composition diversity. In a 5-day online A/B test with 5% traffic on Kuaishou e-commerce, QuaSID-learned SIDs improve ranking GMV-S2 by **2.38%** and bring particularly strong gains on cold-start

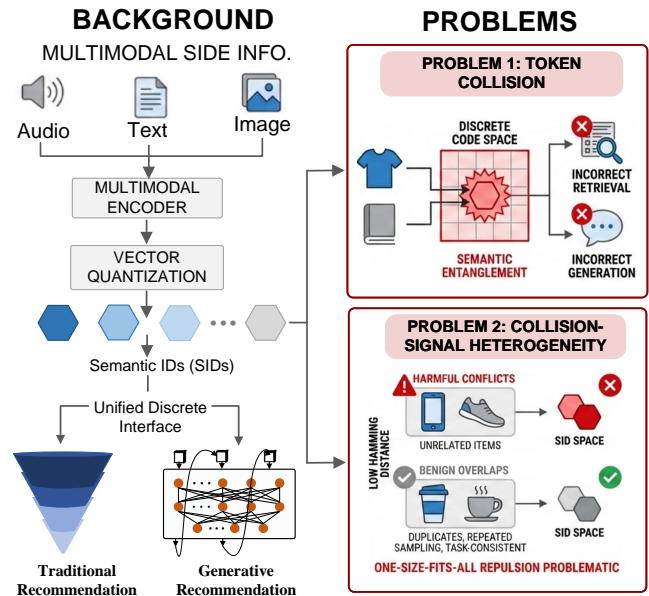


**Figure 1: SID learning in large-scale recommendation: multimodal features are encoded and quantized into SIDs as a unified discrete interface for traditional and generative paradigms. Challenges: token collisions cause semantic entanglement, and overlap signals are heterogeneous (harmful vs. benign), so one-size-fits-all suppression is problematic.**

retrieval, with completed orders improving by up to **6.42%** on the 100vv cold-start segment. Moreover, we show that the HaMR repulsion loss is plug-and-play and consistently enhances a wide range of SID learning frameworks across datasets. The main contributions of this work are as follows:

- We propose QuaSID, a qualification-aware framework for learning collision-qualified SIDs, and introduce HaMR to translate low-Hamming SID overlaps into severity-aware geometric margin constraints in the encoder space.
- We introduce CVPM to qualify collision supervision by masking protocol-induced benign overlaps (e.g., duplicates and constructed positives), yielding a cleaner conflict set for repulsion-based learning.
- We validate QuaSID through extensive offline experiments and large-scale online A/B tests, demonstrating consistent improvements in ranking quality, SID composition diversity, and business-critical metrics.

## 2 Related Work

### 2.1 Vector Quantization for Semantic Tokenization

Vector quantization (VQ) maps continuous embeddings to a finite set of discrete codewords, typically trained with reconstruction objectives and commitment-style regularizers, and optimized via straight-through or relaxed estimators [24]. To expand capacity without inflating a single vocabulary, modern tokenizers often adopt compositional designs: residual vector quantization (RQ)

stacks multiple codebooks to iteratively quantize residuals, achieving strong expressiveness with small per-layer codebooks [14, 32]. Grouped variants further reduce cross-dimension interference and can improve optimization stability and utilization [27]. Beyond architecture, a line of work improves assignment and normalization, refines gradient estimators, and explicitly diagnoses collapse and under-utilization [3, 19, 37]. More recently, Finite Scalar Quantization (FSQ) replaces explicit codebooks with per-dimension scalar quantization over fixed levels, inducing an implicit Cartesian-product codebook and simplifying training [20]. Overall, these advances primarily improve quantization capacity and code usage for generic embedding compression.

While the above tokenizers substantially improve quantization capacity and code usage, they are largely developed under a reconstruction oriented paradigm. In Semantic ID construction, discrete codes serve as identifiers and indexing keys for retrieval and ranking, where the key failure mode is confusability between semantically distinct items. Since reconstruction-dominated VQ objectives only weakly constrain such confusability, collision control is typically indirect and can be misaligned with recommendation needs [6, 11]. This gap motivates incorporating recommendation-aligned supervision and discrete-space diagnostics to explicitly shape the encoder and reduce harmful collisions.

## 2.2 SID-based Recommendation

SID-based recommendation represents each item as a fixed-length sequence of discrete semantic tokens, offering compact, reusable, and index-friendly item representations that avoid vocabulary explosion [15]. This interface has been adopted in both discriminative [18, 23, 26, 30, 34] and generative recommendation systems [2, 8, 35], demonstrating broad applicability across paradigms.

Early SID learning typically follows a projection–quantization–reconstruction pipeline built on VQ/RQ tokenizers [14, 24]. Recent methods make SID learning more task-aware by injecting collaborative signals into code assignment and training objectives, including VQ-Rec [9], LC-Rec [33], RQ-KMeans [35], ETEGRec [16], and LMIndexer [13]. Several works further target collision or assignment imbalance explicitly. SaviorRec [29] integrates Sinkhorn-based entropy-regularized optimal transport to encourage more uniform assignments (see [4] for the Sinkhorn algorithm); LETTER constrains per-codebook  $k$ -means by limiting the maximum number of items per centroid [25]; HiD-VAE adds regularization to penalize excessive code overlap across distinct items [5]. Despite their effectiveness, most collision-aware strategies rely on coarse overlap signals and apply uniform suppression without qualifying what a discrete agreement represents. In large-scale pipelines, low-Hamming overlaps can be heterogeneous, reflecting harmful collisions between unrelated items or benign agreements induced by repeated sampling and task-consistent relations. Indiscriminate suppression can introduce spurious separation and destabilize training, highlighting the need for qualification-aware and severity-adaptive collision control that selects valid conflict pairs and scales repulsion by collision severity.

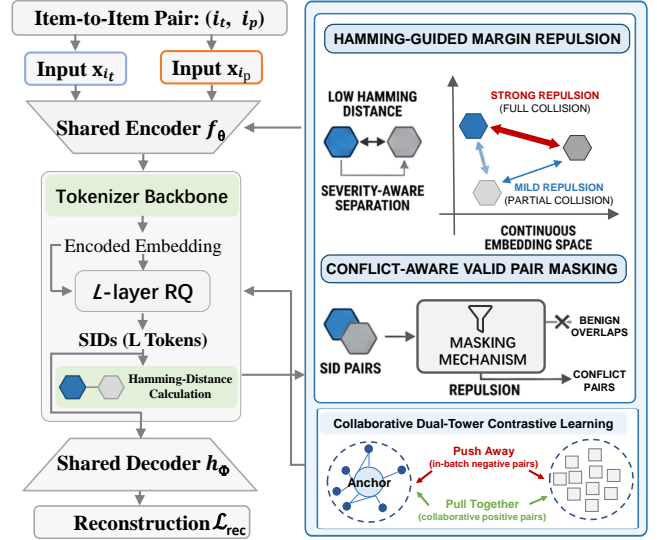


Figure 2: The overall framework of QuaSID.

## 3 Preliminaries

*Notations.* Let  $\mathcal{U}$  and  $\mathcal{I}$  denote the user set and item set, with  $|\mathcal{U}| = N_u$  and  $|\mathcal{I}| = N_i$ . Each item  $i \in \mathcal{I}$  is associated with a multimodal feature vector  $\mathbf{x}_i \in \mathbb{R}^{d_{in}}$ , which may include visual, textual, and audio attributes. Let  $f_\theta(\cdot)$  denote an encoder network that maps the multimodal item feature  $\mathbf{x}_i$  into a continuous latent embedding, defined as:

$$\mathbf{z}_i = f_\theta(\mathbf{x}_i) \in \mathbb{R}^d. \quad (1)$$

We adopt a residual vector quantization scheme with  $L$  codebooks. The  $l$ -th codebook is denoted as  $\mathcal{C}^{(l)} = \{\mathbf{c}_k^{(l)}\}_{k=1}^K$ , where  $K$  is the codebook size. For each layer  $l$ , a discrete index  $s_i^{(l)} \in \{1, \dots, K\}$  is selected, producing a quantized embedding  $\mathbf{q}_i^{(l)} = \mathbf{c}_{s_i^{(l)}}^{(l)}$ . The SID of item  $i$  is represented as a sequence of discrete tokens:

$$\mathbf{s}_i = [s_i^{(1)}, s_i^{(2)}, \dots, s_i^{(L)}] \in \{1, \dots, K\}^L. \quad (2)$$

*Problem definition.* Given a set of multimodal items  $\mathcal{I}$  with their feature vectors  $\{\mathbf{x}_i \mid i \in \mathcal{I}\}$  and a set of observed collaborative item-item pairs  $\mathcal{P} = \{(i_t, i_p)\}$  derived from user interaction logs, our goal is to learn a SID generator

$$g_\theta : \mathbf{x}_i \mapsto \mathbf{s}_i \in \{1, \dots, K\}^L.$$

Formally, we aim to jointly learn the encoder  $f_\theta$ , the codebooks  $\mathcal{C}^{(l)}_{l=1}^L$ , and the discrete assignment mechanism. The goal is to produce collision-qualified SIDs that remain compatible with collaborative signals and can be deployed in both discriminative and generative recommendation systems.

## 4 Method

### 4.1 Overall Framework

*Tokenizer Backbone.* As summarized in Figure 2, QuaSID is an end-to-end SID learner that grounds discrete codes in both multimodal semantics and collaborative signals. Given a collaborative

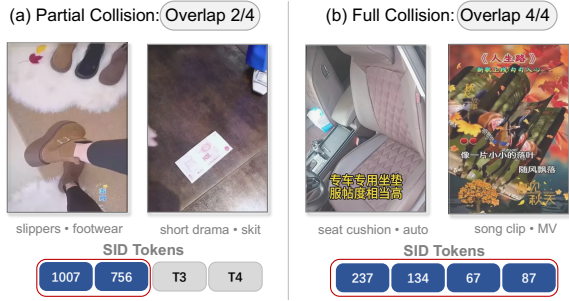


**Figure 3: Representative in-batch collision cases in industrial SID training. (a) Partial collision with 2/4 token overlap. (b) Complete collision with identical 4-token SIDs between semantically dissimilar items.**

item-to-item pair, QuaSID first maps each multimodal input  $\mathbf{x}$  into a continuous embedding via a shared encoder  $f_\theta$ . The embedding is then discretized by an  $L$ -layer residual vector quantizer to produce an  $L$ -token SID  $\mathbf{s}_i$  together with its quantized representation  $\hat{\mathbf{z}}_i$ . To preserve semantic fidelity under discretization, a decoder  $h_\phi$  reconstructs the original feature from  $\hat{\mathbf{z}}_i$ , yielding a reconstruction-based regularization of the discrete interface. QuaSID further introduces (i) masked hamming-guided margin repulsion to suppress harmful in-batch SID collisions, and (ii) collaborative dual-tower contrastive learning to align learned SIDs with downstream behavioral semantics. Concretely, we encode the trigger and target items with a shared encoder  $f_\theta$  as follows:

$$\mathbf{z}_{i_t} = f_\theta(\mathbf{x}_{i_t}), \quad \mathbf{z}_{i_p} = f_\theta(\mathbf{x}_{i_p}). \quad (3)$$

Here  $\mathbf{x}_{i_t}, \mathbf{x}_{i_p} \in \mathbb{R}^{d_{in}}$  are multimodal item features,  $\mathbf{z}_i \in \mathbb{R}^d$  denotes the continuous embedding. For each item  $i$ , we initialize  $\mathbf{r}_i^{(0)} = \mathbf{z}_i$  and iteratively quantize the residual using  $L$  codebooks, yielding the quantized embedding  $\hat{\mathbf{z}}_i$  and SID  $\mathbf{s}_i$ :

$$\mathbf{q}_i^{(l)} = \mathbf{c}_{\mathbf{s}_i^{(l)}}^{(l)}, \quad \mathbf{r}_i^{(l)} = \mathbf{r}_i^{(l-1)} - \mathbf{q}_i^{(l)}, \quad l = 1, \dots, L, \quad (4)$$

$$\hat{\mathbf{z}}_i = \sum_{l=1}^L \mathbf{q}_i^{(l)}, \quad \mathbf{s}_i = [\mathbf{s}_i^{(1)}, \dots, \mathbf{s}_i^{(L)}].$$

We reconstruct the multimodal input from  $\hat{\mathbf{z}}_i$  using a decoder  $h_\phi$ :  $\hat{\mathbf{x}}_i = h_\phi(\hat{\mathbf{z}}_i)$ . The backbone is trained with a reconstruction term and the standard residual-quantization objective:

$$\mathcal{L}_{\text{rec}} = \frac{1}{|\mathcal{B}|} \sum_{i \in \mathcal{B}} \ell_{\text{rec}}(\hat{\mathbf{x}}_i, \mathbf{x}_i), \quad (5a)$$

$$\mathcal{L}_{\text{rq}} = \frac{1}{|\mathcal{B}|} \sum_{i \in \mathcal{B}} \sum_{l=1}^L \left( \|\text{sg}[\mathbf{r}_i^{(l-1)}] - \mathbf{q}_i^{(l)}\|_2^2 + \beta \|\mathbf{r}_i^{(l-1)} - \text{sg}[\mathbf{q}_i^{(l)}]\|_2^2 \right), \quad (5b)$$

where  $\ell_{\text{rec}}(\cdot, \cdot)$  is instantiated as the  $L_2$  loss,  $\text{sg}[\cdot]$  denotes stop-gradient, and  $\beta$  controls the commitment strength.

**Collaborative Dual-Tower Contrastive Alignment.** Beyond reconstruction and quantization, QuaSID injects collaborative semantics into tokenization via a dual-tower contrastive objective defined

on observed item–item co-engagement pairs (denoted as trigger–target pairs  $(i_t, i_p)$ ). In this work, we adopt Swing [28] to construct such collaborative pairs, together with data cleaning and filtering strategies to ensure high-quality supervision.

Given a batch of normalized encoded trigger embeddings  $\{\mathbf{e}_t^m\}_{m=1}^B$  and target embeddings  $\{\mathbf{e}_p^n\}_{n=1}^B$ , we compute the scaled similarities across the mini-batch:

$$\mathbf{S}_{m,n} = \frac{(\mathbf{e}_t^m)^\top \mathbf{e}_p^n}{\tau}, \quad (6)$$

where  $\tau$  is a temperature hyperparameter. The contrastive learning objective follows the InfoNCE formulation:

$$\mathcal{L}_{\text{cl}} = -\frac{\lambda_{\text{cl}}}{B} \sum_{m=1}^B \log \frac{\exp(\mathbf{S}_{m,m})}{\sum_{n=1}^B \mathbb{I}[M_{m,n} = 1] \exp(\mathbf{S}_{m,n})}, \quad (7)$$

where  $\lambda_{\text{cl}}$  is the contrastive loss weight and  $M_{m,n}$  is a masking indicator. To reduce false-negative bias, we set  $M_{m,n} = 0$  for  $n \neq m$  when  $\text{id}(\mathbf{e}_t^m) = \text{id}(\mathbf{e}_p^n)$ , and  $M_{m,n} = 1$  otherwise. This task-oriented signal complements semantic reconstruction by encouraging SIDs to preserve behaviorally meaningful proximity.

## 4.2 Hamming-guided Margin Repulsion with Conflict-Aware Masking

A core component of QuaSID is **HaMR**, a mask-aware repulsion mechanism that converts *in-batch low-Hamming SID overlaps* into explicit geometric margin constraints on the encoder space. Under a well-utilized discrete space, it is statistically uncommon for two distinct instances in the same mini-batch to share many SID tokens; hence unusually low Hamming distances within a mini-batch suggest insufficient separation in the learned representations. Figure 3 presents representative collision cases observed in real-world training scenarios. However, mini-batches also contain overlaps that should *not* be repelled by design, such as duplicate occurrences of the same underlying item and the constructed item–item positives used for the contrastive objective. Therefore, QuaSID employs Conflict-Aware Valid Pair Masking (CVPM) to address the *heterogeneity* of apparent in-batch overlaps by masking these protocol-induced non-conflict pairs before applying repulsion, yielding a cleaner set of candidate conflict pairs for HaMR.

**4.2.1 Conflict-Aware Valid Pair Masking (CVPM).** We propose CVPM to *qualify* collision supervision by masking item–item pairs whose discrete overlaps are likely benign, thereby restricting repulsion to a cleaner and more informative subset of candidate conflict pairs. Let the mini-batch be formed by concatenating triggers and targets, yielding  $2B$  instances indexed by  $i \in \{1, \dots, 2B\}$ , and let  $\text{id}(i)$  denote the underlying item ID of instance  $i$ .

(1) Collaborative-positive mask: we exclude constructed collaborative positives  $(i_t, i_p)$  used by the contrastive objective from collision supervision; otherwise, repulsion would directly contradict task-aligned similarity:

$$\mathbf{M}_{ij}^{\text{izi}} = \begin{cases} 0, & (i \leq B \wedge j = i + B) \vee (j \leq B \wedge i = j + B), \\ 1, & \text{otherwise.} \end{cases}$$

(2) Same-item exclusion mask: we exclude pairs that correspond to the same underlying item ID, covering both self-pairs ( $i = j$ ) and

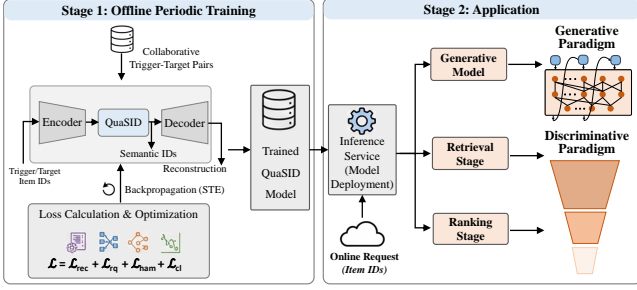


Figure 4: QuaSID deployment and application pipeline.

duplicate occurrences caused by repeated sampling. This avoids treating repeated exposures as collisions:

$$\mathbf{M}_{ij}^{\text{item}} = \mathbb{I}[\text{id}(i) \neq \text{id}(j)].$$

Combining the two masks yields a pairwise filter for collision supervision, retaining only the qualified in-batch pairs  $(i, j)$ :

$$\mathbf{M} = \mathbf{M}^{\text{id}} \odot \mathbf{M}^{\text{item}}, \quad (8)$$

where  $\odot$  denotes the element-wise (Hadamard) product. We incorporate  $\mathbf{M}$  as a binary gate in the HaMR loss to mask out excluded in-batch pairs  $(i, j)$  during repulsion computation.

**4.2.2 Hamming-guided margin repulsion (HaMR).** We view unexpectedly low-Hamming SID agreements as conflict signals. Accordingly, conditioned on the CVPM valid-pair mask  $\mathbf{M}$ , we enforce a severity-aware cosine-distance margin between the normalized encoder embeddings to suppress harmful collisions. Let  $\mathbf{s}_i \in \{1, \dots, K\}^L$  denote the SID and  $\mathbf{e}_i = \mathbf{z}_i / \|\mathbf{z}_i\|_2$  the normalized embedding. We define the pairwise Hamming-distance matrix  $\mathbf{H} \in \mathbb{N}^{2B \times 2B}$  and the cosine-distance matrix  $\mathbf{D} \in \mathbb{R}^{2B \times 2B}$  by

$$\mathbf{H}_{ij} = d_H(i, j) = \sum_{l=1}^L \mathbb{I}[s_i^{(l)} \neq s_j^{(l)}], \quad (9)$$

$$\mathbf{D}_{ij} = d_c(i, j) = 1 - \mathbf{e}_i^\top \mathbf{e}_j. \quad (10)$$

Based on the Hamming distance, we distinguish between two types of collisions: *full collision* and *partial collision*. This distinction allows us to adaptively control the penalty strength according to the severity of the collision. Intuitively, a full collision represents a more problematic case and thus warrants a stronger penalty. Using the masks defined above, we partition candidate pairs into two sets:

$$\begin{aligned} \Omega_{\text{full}} &= \{(i, j) \mid \mathbf{H}_{ij} = 0 \text{ and } \mathbf{M}_{ij} = 1\}, \\ \Omega_{\text{partial}} &= \{(i, j) \mid 0 < \mathbf{H}_{ij} \leq R \text{ and } \mathbf{M}_{ij} = 1\}, \end{aligned}$$

where  $R$  is a hyperparameter that determines the Hamming radius for considering partial collisions. For each pair  $(i, j)$  we penalize small cosine distances via margin-based hinge losses:

$$\mathcal{L}_{\text{full}}(i, j) = \max(0, m_{\text{full}} - \mathbf{D}_{ij}), \quad (11)$$

$$\mathcal{L}_{\text{partial}}(i, j) = \max(0, m_{\text{partial}} - \mathbf{D}_{ij}), \quad (12)$$

Table 1: Dataset statistics used in the experiments.

Dataset	#Users	#Items	#Interactions
Amazon-Beauty	22,363	12,101	1,048,296
Amazon-Toys	19,412	11,924	905,253

where  $m_{\text{full}}$  and  $m_{\text{partial}}$  are predefined margins with  $m_{\text{full}} \geq m_{\text{partial}}$ . The masked hamming-guided margin is therefore computed as:

$$\begin{aligned} \mathcal{L}_{\text{HaMR}} &= \frac{\lambda_{\text{full}}}{|\Omega_{\text{full}}| + \epsilon} \sum_{(i,j) \in \Omega_{\text{full}}} \mathcal{L}_{\text{full}}(i, j) \\ &+ \frac{\lambda_{\text{partial}}}{|\Omega_{\text{partial}}| + \epsilon} \sum_{(i,j) \in \Omega_{\text{partial}}} \mathcal{L}_{\text{partial}}(i, j), \end{aligned} \quad (13)$$

where  $\lambda_{\text{full}}$  and  $\lambda_{\text{partial}}$  are weighting coefficients and  $\epsilon > 0$  is a small constant for numerical stability.

Eq. (13) imposes geometric constraints on the encoder space for the selected pairs: for any  $(i, j) \in \Omega_{\text{full}}$  (resp.  $\Omega_{\text{partial}}$ ), achieving zero hinge loss implies  $d_c(i, j) \geq m_{\text{full}}$  (resp.  $d_c(i, j) \geq m_{\text{partial}}$ ). With CVPM filtering constructed positives and same-ID pairs, repulsion focuses on discretely similar item pairs that are unlikely to be benign artifacts, increasing their angular separation before quantization. Over training, such targeted separation reshapes the continuous embedding space and reduces collision frequency, without enforcing uniform repulsion across all item pairs.

### 4.3 System Deployment and Application

QuaSID has been successfully deployed and applied on KuaiShou’s recommendation system, as illustrated in Figure 4. The deployment and application pipeline consists of the following key stages: (1) Offline periodic training: Based on the production speed of the trigger-target pair, we train our model periodically using the overall optimization objective:

$$\mathcal{L} = \mathcal{L}_{\text{rec}} + \mathcal{L}_{\text{rq}} + \mathcal{L}_{\text{HaMR}} + \mathcal{L}_{\text{cl}}. \quad (14)$$

All components are trained end-to-end using backpropagation, where the discrete code assignments are optimized via the straight-through estimator (STE) to enable differentiable learning. (2) Application for retrieval and ranking stage: The trained QuaSID is deployed as an inference service to project item ids into SIDs. QuaSID-learned SIDs correspond to a new lookup table and are used in both retrieval and ranking stages. The retrieval stage including conventional retrieval and SID-based generative retrieval. At the ranking stage, SIDs are used to derive cross features and matching side features, serving as lightweight semantic signals that augment the existing feature set.

## 5 Experiment

### 5.1 Experimental Setup

**5.1.1 Datasets.** We use two public benchmarks for offline evaluation and an industrial dataset for online A/B tests, as detailed below. **Public Datasets.** For offline generative recommendation evaluation, we use the widely adopted Amazon 2018 review datasets<sup>1</sup>.

<sup>1</sup><https://nijianmo.github.io/amazon/>

**Table 2: Performance comparison on Amazon-Beauty and Amazon-Toys. Bold denotes the best result, and underlined denotes the second-best result.**

Tokenizer	Amazon-Beauty					Amazon-Toys				
	HR@5	HR@10	NDCG@5	NDCG@10	Entropy	HR@5	HR@10	NDCG@5	NDCG@10	Entropy
RQ-VAE	0.0225	0.0300	0.0171	0.0195	9.3075	0.0206	0.0256	0.0164	0.0180	9.3068
Improved VQGAN	0.0232	0.0304	0.0167	0.0189	9.3569	0.0196	0.0245	0.0157	0.0172	9.3313
GRVQ	0.0222	0.0302	0.0161	0.0187	9.2755	0.0195	0.0242	0.0158	0.0173	9.2101
RQ-OPQ	0.0205	0.0271	0.0159	0.0180	9.3368	0.0228	0.0278	0.0179	0.0195	9.3521
RQ-VAE-Rotation	0.0236	0.0308	<u>0.0175</u>	0.0198	9.3455	0.0203	0.0257	0.0167	0.0187	9.3290
SimRQ	0.0231	0.0297	0.0172	0.0193	9.3526	0.0220	0.0279	0.0171	0.0190	9.3688
RQ-Kmeans	<u>0.0254</u>	<u>0.0379</u>	0.0171	<u>0.0211</u>	<u>9.3793</u>	<u>0.0260</u>	<u>0.0347</u>	<u>0.0190</u>	<u>0.0213</u>	9.3460
QuaSID	<b>0.0277</b>	<b>0.0392</b>	<b>0.0193</b>	<b>0.0230</b>	<b>9.3901</b>	<b>0.0266</b>	<b>0.0366</b>	<b>0.0193</b>	<b>0.0225</b>	<b>9.3794</b>

**Table 3: Effect of HaMR ( $\mathcal{L}_{\text{HaMR}}$ ) on different semantic ID learning methods.**

Tokenizer	Amazon-Beauty					Amazon-Toys				
	HR@5	HR@10	NDCG@5	NDCG@10	Entropy	HR@5	HR@10	NDCG@5	NDCG@10	Entropy
RQ-VAE	0.0225	0.0300	0.0171	0.0195	9.3075	0.0206	0.0256	0.0164	0.0180	9.3068
+ $\mathcal{L}_{\text{HaMR}}$	0.0246 $\uparrow$ 9.3%	0.0348 $\uparrow$ 16.0%	0.0182 $\uparrow$ 6.4%	0.0215 $\uparrow$ 10.3%	9.3971 $\uparrow$ 1.0%	0.0239 $\uparrow$ 16.0%	0.0290 $\uparrow$ 13.3%	0.0187 $\uparrow$ 14.0%	0.0203 $\uparrow$ 12.8%	9.3795 $\uparrow$ 0.8%
Improved VQGAN	0.0232	0.0304	0.0167	0.0189	9.3569	0.0196	0.0245	0.0157	0.0172	9.3313
+ $\mathcal{L}_{\text{HaMR}}$	0.0257 $\uparrow$ 10.8%	0.0340 $\uparrow$ 11.8%	0.0192 $\uparrow$ 15.0%	0.0218 $\uparrow$ 15.3%	9.3974 $\uparrow$ 0.4%	0.0239 $\uparrow$ 21.8%	0.0301 $\uparrow$ 22.8%	0.0187 $\uparrow$ 18.9%	0.0207 $\uparrow$ 20.1%	9.3797 $\uparrow$ 0.5%
GRVQ	0.0222	0.0302	0.0161	0.0187	9.2755	0.0195	0.0242	0.0158	0.0173	9.2101
+ $\mathcal{L}_{\text{HaMR}}$	0.0251 $\uparrow$ 13.1%	0.0341 $\uparrow$ 12.9%	0.0181 $\uparrow$ 12.4%	0.0210 $\uparrow$ 12.3%	9.3986 $\uparrow$ 1.3%	0.0232 $\uparrow$ 19.0%	0.0284 $\uparrow$ 17.4%	0.0186 $\uparrow$ 17.7%	0.0202 $\uparrow$ 16.8%	9.3808 $\uparrow$ 1.9%
RQ-OPQ	0.0205	0.0271	0.0159	0.0180	9.3368	0.0228	0.0278	0.0179	0.0195	9.3521
+ $\mathcal{L}_{\text{HaMR}}$	0.0241 $\uparrow$ 17.6%	0.0317 $\uparrow$ 17.0%	0.0179 $\uparrow$ 12.5%	0.0203 $\uparrow$ 12.5%	9.3973 $\uparrow$ 0.6%	0.0227 $\downarrow$ 0.4%	0.0280 $\uparrow$ 0.7%	0.0180 $\uparrow$ 0.6%	0.0197 $\uparrow$ 1.0%	9.3798 $\uparrow$ 0.3%
RQ-VAE-Rotation	0.0236	0.0308	0.0175	0.0198	9.3455	0.0203	0.0257	0.0167	0.0187	9.3290
+ $\mathcal{L}_{\text{HaMR}}$	0.0242 $\uparrow$ 2.5%	0.0327 $\uparrow$ 6.2%	0.0175	0.0202 $\uparrow$ 2.0%	9.3939 $\uparrow$ 0.5%	0.0219 $\uparrow$ 7.9%	0.0272 $\uparrow$ 5.8%	0.0174 $\uparrow$ 3.9%	0.0191 $\uparrow$ 2.0%	9.3765 $\uparrow$ 0.5%
SimRQ	0.0231	0.0297	0.0172	0.0193	9.3526	0.0220	0.0279	0.0171	0.0190	9.3688
+ $\mathcal{L}_{\text{HaMR}}$	0.0238 $\uparrow$ 3.0%	0.0323 $\uparrow$ 8.8%	0.0174 $\uparrow$ 1.2%	0.0201 $\uparrow$ 4.1%	9.3977 $\uparrow$ 0.5%	0.0227 $\uparrow$ 3.2%	0.0283 $\uparrow$ 1.4%	0.0182 $\uparrow$ 6.4%	0.0200 $\uparrow$ 5.3%	9.3793 $\uparrow$ 0.1%

Specifically, we select the *Beauty* and *Toys & Games* subsets to evaluate our method. Following prior work [7], we apply a standard *5-core* filtering procedure, discarding users and items with fewer than five interactions. We then adopt a leave-one-out strategy to split each dataset into training, validation, and test sets. Item textual fields include *Title*, *Brand*, *Categories*, and *Price*. We concatenate these fields and extract semantic item embeddings using Sentence-T5-XXL [21]. The dataset statistics are shown in Table 1. **Industrial Dataset.** On an industrial dataset from the Kuaishou platform, we perform online A/B tests to evaluate QuaSID in both generative retrieval and discriminative pipelines (including retrieval and ranking). Each item is associated with rich multimodal side information, including textual descriptions, automatic speech recognition (ASR) transcripts, and key-frame images. Multimodal item embeddings are extracted using multimodal large language models.

**5.1.2 Baselines.** For offline experiments, we compare QuaSID with strong VQ-based tokenizers, including **RQ-VAE** [14], **GRVQ** [27], **Improved VQGAN** [31], **RQ-VAE-Rotation** [6], **SimRQ** [37], **RQ-OPQ** [2], and **RQ-Kmeans** [18]. Due to space, detailed baseline descriptions are deferred to Appendix A.1.

**5.1.3 Evaluation Metrics.** For offline evaluation on public datasets, we report HitRate@ $K$  and NDCG@ $K$  with  $K \in \{5, 10\}$  as the ranking metrics. We additionally report the entropy of *SID compositions* to measure the diversity of discrete ID assignments. Let  $p(\mathbf{s})$  denote the empirical frequency of an SID sequence  $\mathbf{s}$  over the item corpus; we compute  $\mathcal{E}_{\text{SID}} = -\sum_{\mathbf{s}} p(\mathbf{s}) \log p(\mathbf{s})$ , where larger values indicate more diverse SIDs (i.e., fewer duplicated compositions). For online A/B tests on the industrial dataset, we report business metrics as described in Section 5.4.

**5.1.4 Implementation Details.** For offline experiments, we employ TIGER [22] as the generative recommendation backbone for all methods, and keep identical model configurations across QuaSID and baselines. For the codebook setting, we set  $L = 3$  and  $K = 256$  in offline experiments, while in industrial experiments we use  $L = 4$  and  $K = 1024$ . All results are averaged over five random seeds. Additional training details and hyperparameter ranges are provided in Appendix A.2.

## 5.2 Overall Performance

We compare QuaSID with multiple baselines on the public datasets under the offline generative recommendation setting. The results

**Table 4: Online A/B test results on Kuaishou e-commerce. Relative uplifts (%) brought by integrating QuaSID-learned SIDs into retrieval and ranking.**

Setting	Completed Orders	GMV-S1	GMV-S2
Generative Retrieval	+0.21%	+1.03%	+0.55%
Ranking	+0.20%	+1.44%	+2.38%
	Completed Orders	GMV	GPM
Retrieval	+1.09%	+1.69%	+3.25%
Retrieval <sub>100vv</sub>	+6.42%	+4.67%	+0.21%
Retrieval <sub>600vv</sub>	+4.69%	+3.11%	+0.53%
Ranking <sub>100vv</sub>	+1.77%	+4.10%	+2.99%
Ranking <sub>600vv</sub>	+2.64%	+3.88%	+2.78%

are shown in Table 2. All improvements are statistically significant ( $p < 0.05$ ). Based on the results, we have the following observations:

- As shown in Table 2, QuaSID consistently achieves the best performance on all ranking metrics (HR@K and NDCG@K) across both Amazon-Beauty and Amazon-Toys. The improvements are substantial and consistent compared to strong VQ-based baselines, indicating that collision-reduced and collaboration-aware SID learning translates into superior downstream recommendation quality.
- QuaSID also attains the highest entropy on both datasets, indicating more diverse discrete ID assignments and better utilization of the discrete SID space. Together with the ranking improvements, this indicates that the proposed framework enhances task performance while maintaining a compact and efficient discrete interface; by integrating task-aligned supervision with collision-aware regularization, QuaSID jointly improves SID discriminability, task alignment, and SID assignment diversity within a single end-to-end learning objective.

*Entropy–ranking quality relationship.*  $\mathcal{E}_{\text{SID}}$  measures the diversity of SID compositions (i.e., how evenly the discrete space is utilized). Across tokenizers, higher  $\mathcal{E}_{\text{SID}}$  generally coincides with better ranking metrics, and the overall correlation is positive when aggregating Amazon-Beauty and Amazon-Toys (Pearson  $r$  around 0.65, Spearman  $\rho$  around 0.72; statistically significant). However, entropy is not a sufficient predictor of ranking quality. A higher  $H_{\text{SID}}$  mainly reflects fewer duplicated compositions, while HR/NDCG further depends on whether the discrete interface preserves task-relevant semantics. For example, on Amazon-Toys, SimRQ attains high entropy (9.3688, second-best) but underperforms RQ-Kmeans on NDCG@10 (0.0190 vs. 0.0213) despite RQ-Kmeans having lower entropy (9.3460).

### 5.3 Plug-and-Play Analysis of HaMR

To evaluate the generalization ability of the proposed HaMR loss ( $\mathcal{L}_{\text{HaMR}}$ ), we conduct a controlled study where all training settings and hyperparameters are kept identical, and we add the HaMR loss as an auxiliary objective to a diverse set of semantic ID learning baselines. The results are summarized in Table 3. Note that RQ-Kmeans is excluded from Table 3, as its tokenizer is not trained

under the same end-to-end, gradient-based optimization framework as the tokenizers evaluated in this study. Based on the empirical evidence, we draw the following observations:

- As shown in Table 3, adding the HaMR loss improves the downstream ranking metric NDCG@10 by up to 15.3% (Beauty) and 20.1% (Toys), while also increasing entropy by around 0.1%–1.9%. This demonstrates that the proposed hamming-guided margin repulsion is model-agnostic and can be seamlessly integrated as a plug-and-play component to enhance semantic ID discriminability, collision reduction, and SID assignment diversity simultaneously.
- By comparing Table 3 with the overall performance of QuaSID in Table 2, we observe a contrast: while adding  $\mathcal{L}_{\text{HaMR}}$  to baselines often results in higher entropy than QuaSID, their ranking metrics remain consistently inferior to QuaSID. This suggests that although hamming-guided repulsion is highly effective in improving SID-composition diversity and SID structure, it alone is insufficient to fully optimize downstream recommendation performance in the offline generative setting. The additional gains achieved by QuaSID can be likely related to its task-aware training module, which aligns semantic IDs with recommendation objectives. Together, these results highlight that  $\mathcal{L}_{\text{HaMR}}$  and contrastive task supervision are complementary: the former improves discrete representation quality, while the latter ensures effective downstream task alignment.

### 5.4 Online A/B Test

We further evaluate QuaSID through large-scale online A/B testing in the e-commerce recommendation scenario of the Kuaishou platform. Approximately 5% of online traffic (covering over 20 million users) is randomly assigned to the treatment group for 5 days. We report Completed Orders (CO), GMV (including scenario-specific GMV, i.e., GMV-S1/GMV-S2), and GPM (GMV per mille exposures) in Table 4; 100vv and 600vv denote cold-start videos with fewer than 100 and 600 views, respectively, within the first 48 hours. All results are statistically significant.

*Retrieval.* We evaluate both **generative retrieval** and the **conventional discriminative retrieval** pipeline, together with their cold-start subsets. As shown in Table 4, replacing the tokenizer with QuaSID-learned SIDs improves CO and GMV-related metrics across settings, with substantially larger gains under sparse feedback. In generative retrieval, QuaSID yields +0.21% CO and +1.03% / +0.55% GMV-S1/GMV-S2. The effect is amplified on cold-start traffic, where CO increases by +6.42% (100vv) and +4.69% (600vv). GPM follows the same trend.

*Ranking.* QuaSID also delivers stable improvements when integrated into **discriminative ranking models**. We observe +2.38% GMV-S2, accompanied by +1.44% GMV-S1 and +0.20% CO. While the absolute uplifts are smaller than those in retrieval, the gains remain consistently positive across scenarios, and cold-start segments still benefit noticeably. Overall, these results demonstrate that QuaSID-learned SIDs can be deployed in production ranking and retrieval stacks and translate into measurable business impact.

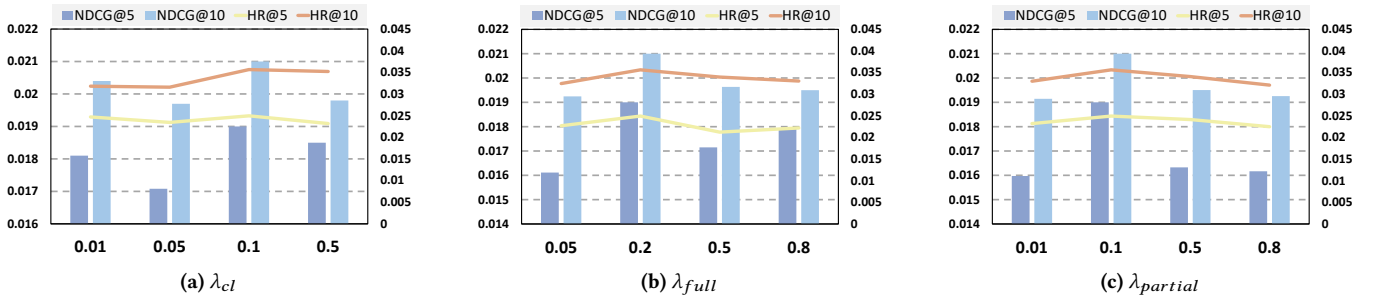


**Figure 5: Hyperparameter sensitivity analysis of QuaSID on the Amazon-Beauty dataset. The bars indicate NDCG@K (left y-axis), while the curves denote HR@K (right y-axis). In each subfigure, one hyperparameter is varied while all others are fixed to their default values.**

**Table 5: Ablation study results on Amazon-Beauty and Amazon-Toys datasets.**

Tokenizer	Amazon-Beauty		Amazon-Toys	
	HR@5	NDCG@5	HR@5	NDCG@5
QuaSID	0.0277	0.0193	0.0266	0.0193
w/o CVPM	0.0263	0.0181	0.0264	0.0190
w/o HaMR	0.0254	0.0170	0.0261	0.0189

## 5.5 Ablation Study

We conduct ablation studies on the Amazon-Beauty and Amazon-Toys datasets to examine the effectiveness of the key components in QuaSID. Specifically, we evaluate: (i) CVPM, which qualifies collision supervision by masking pairs that are likely to reflect benign overlaps; (ii) the hamming-guided margin repulsion loss  $\mathcal{L}_{HaMR}$  for collision suppression. Results are reported in Table 5.

*Effect of CVPM.* To assess whether valid-pair masking is necessary for reliable collision supervision, we remove CVPM while keeping the remaining objectives unchanged (denoted as w/o CVPM). As shown in Table 5, this variant consistently degrades performance on both datasets, with a more noticeable drop on Amazon-Beauty. This supports our motivation that apparent in-batch collisions are heterogeneous and require qualification. Without CVPM, benign overlaps can be mistakenly included in the repulsion set, introducing spurious separation that pushes apart semantically aligned items and degrades downstream performance.

*Effect of HaMR.* To evaluate the role of collision reduction, we remove HaMR from QuaSID (denoted as w/o HaMR). As shown in Table 5, this variant consistently underperforms the full model across both datasets and evaluation metrics. These results indicate that explicitly penalizing unreasonable SID collisions is critical for preserving semantic discriminability in the discrete token space.

## 5.6 Hyperparameter Sensitivity Analysis

We evaluate QuaSID’s sensitivity to key hyperparameters on Amazon-Beauty, focusing on the collaborative contrastive weight  $\lambda_{cl}$  and the repulsion weights for full and partial SID collisions,  $\lambda_{full}$  and  $\lambda_{partial}$ . Each experiment varies one hyperparameter while keeping

the others at default values. Figure 5 reports NDCG@K (bar plots, left y-axis) and HR@K (line plots, right y-axis).

*Effect of  $\lambda_{cl}$ .*  $\lambda_{cl}$  controls the strength of collaborative supervision that aligns SIDs with behavioral signals. Increasing  $\lambda_{cl}$  from 0.01 to 0.1 consistently improves performance, with HR@10 and NDCG@10 peaking around 0.1, suggesting that moderate contrastive regularization complements reconstruction/quantization by injecting collaborative semantics. Further increasing  $\lambda_{cl}$  to 0.5 degrades performance, indicating that overly strong contrastive forces can dominate optimization and conflict with discretization and collision mitigation.

*Effect of  $\lambda_{full}$ .*  $\lambda_{full}$  penalizes full SID collisions (zero Hamming distance), i.e., the most severe ambiguity. The best results occur at  $\lambda_{full} = 0.2$ . Smaller values under-penalize full collisions and reduce ranking quality, while larger values also hurt performance, likely because excessive repulsion distorts the representation space and weakens semantic generalization.

*Effect of  $\lambda_{partial}$ .*  $\lambda_{partial}$  weights penalties for near-collisions within a Hamming radius  $R = 1$ . Performance improves as  $\lambda_{partial}$  increases from 0.01 to 0.1, implying that mild near-collision repulsion alleviates local codebook overcrowding. However, larger values (0.5, 0.8) consistently reduce HR and NDCG, suggesting that over-penalizing partial collisions can unnecessarily separate semantically related items that naturally share some tokens.

## 6 Conclusion and Future Work

We investigated SIDs for multimodal items and identified two key obstacles: token collisions and collision-signal heterogeneity during training, where discrete overlaps may conflate harmful conflicts with benign, task-consistent relations. We proposed QuaSID, integrating HaMR for severity-aware margin repulsion, CVPM to filter same-item pairs and constructed collaborative positives from collision supervision, and an auxiliary dual-tower contrastive loss to inject collaboration signals into tokenization. Extensive offline benchmarks and large-scale online A/B tests show consistent gains across metrics. Future work will further study collision-signal heterogeneity by automatically separating benign overlaps from true semantic conflicts and learning task-conditional qualification policies for when (and how strongly) to repel collisions.

## References

- [1] Xingyan Bin, Jianfei Cui, Wujie Yan, Zhichen Zhao, Xintian Han, Chongyang Yan, Feng Zhang, Xun Zhou, Xiao Yang, and Zuotao Liu. 2025. Real-time Indexing for Large-scale Recommendation by Streaming Vector Quantization Retriever. In *Proceedings of the 31st ACM SIGKDD Conference on Knowledge Discovery and Data Mining, V2, KDD 2025, Toronto ON, Canada, August 3-7, 2025*. ACM, 4273–4283. <https://doi.org/10.1145/3711896.3737259>
- [2] Ben Chen, Xian Guo, Siyuan Wang, Zihan Liang, Yue Lv, Yufei Ma, Xinlong Xiao, Bowen Xue, Xuxin Zhang, Ying Yang, Huangyu Dai, Xing Xu, Tong Zhao, Mingcan Peng, Xiaoyang Zheng, Chao Wang, Qihang Zhao, Zhixin Zhai, Yang Zhao, Bochao Liu, Jingshan Lv, Xiao Liang, Yuqing Ding, Jing Chen, Chenyi Lei, Wenwu Ou, Han Li, and Kun Gai. 2025. OneSearch: A Preliminary Exploration of the Unified End-to-End Generative Framework for E-commerce Search. *CoRR* abs/2509.03236 (2025). <https://doi.org/10.48550/ARXIV.2509.03236> arXiv:2509.03236
- [3] Chung-Cheng Chiu, James Qin, Yu Zhang, Jiahui Yu, and Yonghui Wu. 2022. Self-supervised learning with random-projection quantizer for speech recognition. In *International Conference on Machine Learning, ICML 2022, 17-23 July 2022, Baltimore, Maryland, USA (Proceedings of Machine Learning Research, Vol. 162)*. PMLR, 3915–3924. <https://proceedings.mlr.press/v162/chiu22a.html>
- [4] Marco Cuturi. 2013. Sinkhorn Distances: Lightspeed Computation of Optimal Transport. In *Advances in Neural Information Processing Systems 26: 27th Annual Conference on Neural Information Processing Systems 2013. Proceedings of a meeting held December 5-8, 2013, Lake Tahoe, Nevada, United States*. 2292–2300.
- [5] Dengzhao Fang, Jingtong Gao, Chengcheng Zhu, Yu Li, Xiangyu Zhao, and Yi Chang. 2025. HiD-VAE: Interpretable Generative Recommendation via Hierarchical and Disentangled Semantic IDs. *CoRR* abs/2508.04618 (2025). <https://doi.org/10.48550/ARXIV.2508.04618> arXiv:2508.04618
- [6] Christopher Fifty, Ronald Guenther Junkins, Dennis Duan, Aniketh Iyengar, Jerry Weihong Liu, Ehsan Amid, Sebastian Thrun, and Christopher Ré. 2025. Restructuring Vector Quantization with the Rotation Trick. In *The Thirteenth International Conference on Learning Representations, ICLR 2025, Singapore, April 24-28, 2025*. OpenReview.net. <https://openreview.net/forum?id=GmWRl2e9Y1>
- [7] Shijie Geng, Shuchang Liu, Zuohui Fu, Yingqiang Ge, and Yongfeng Zhang. 2022. Recommendation as Language Processing (RLP): A Unified Pretrain, Personalized Prompt & Predict Paradigm (P5). In *RecSys '22: Sixteenth ACM Conference on Recommender Systems, Seattle, WA, USA, September 18 - 23, 2022*. ACM, 299–315. <https://doi.org/10.1145/3523227.3546767>
- [8] Ruidong Han, Bin Yin, Shangyu Chen, He Jiang, Fei Jiang, Xiang Li, Chi Ma, Mincong Huang, Xiaoquan Li, Chunzhen Jing, Yueming Han, MengLei Zhou, Lei Yu, Chuan Liu, and Wei Lin. 2025. MTGR: Industrial-Scale Generative Recommendation Framework in Meituan. In *Proceedings of the 34th ACM International Conference on Information and Knowledge Management, CIKM 2025, Seoul, Republic of Korea, November 10-14, 2025*. ACM, 5731–5738. <https://doi.org/10.1145/3746252.3761565>
- [9] Yupeng Hou, Zhankui He, Julian J. McAuley, and Wayne Xin Zhao. 2023. Learning Vector-Quantized Item Representation for Transferable Sequential Recommenders. In *Proceedings of the ACM Web Conference 2023, WWW 2023, Austin, TX, USA, 30 April 2023 - 4 May 2023*. ACM, 1162–1171. <https://doi.org/10.1145/3543507.3583434>
- [10] Yupeng Hou, Jiacheng Li, Ashley Shin, Jinsung Jeon, Abhishek Santhanam, Wei Shao, Kaveh Hassani, Ning Yao, and Julian J. McAuley. 2025. Generating Long Semantic IDs in Parallel for Recommendation. In *Proceedings of the 31st ACM SIGKDD Conference on Knowledge Discovery and Data Mining, V2, KDD 2025, Toronto ON, Canada, August 3-7, 2025*. ACM, 956–966. <https://doi.org/10.1145/3711896.3736979>
- [11] Eric Jang, Shixiang Gu, and Ben Poole. 2017. Categorical Reparameterization with Gumbel-Softmax. In *5th International Conference on Learning Representations, ICLR 2017, Toulon, France, April 24-26, 2017, Conference Track Proceedings*. OpenReview.net. <https://openreview.net/forum?id=rkE3y85ee>
- [12] Jian Jia, Jingtong Gao, Ben Xue, Junhao Wang, Qingpeng Cai, Quan Chen, Xiangyu Zhao, Peng Jiang, and Kun Gai. 2025. From Principles to Applications: A Comprehensive Survey of Discrete Tokenizers in Generation, Comprehension, Recommendation, and Information Retrieval. *CoRR* abs/2502.12448 (2025). <https://doi.org/10.48550/ARXIV.2502.12448> arXiv:2502.12448
- [13] Bowen Jin, Hansi Zeng, Guoyin Wang, Xiusi Chen, Tianxin Wei, Ruirui Li, Zhengyang Wang, Zheng Li, Yang Li, Hanqing Lu, Suhang Wang, Jiawei Han, and Xianfeng Tang. 2024. Language Models as Semantic Indexers. In *Forty-first International Conference on Machine Learning, ICML 2024, Vienna, Austria, July 21-27, 2024*. OpenReview.net.
- [14] Doyup Lee, Chihyeon Kim, Saehoon Kim, Minsu Cho, and Wook-Shin Han. 2022. Autoregressive Image Generation using Residual Quantization. In *IEEE/CVF Conference on Computer Vision and Pattern Recognition, CVPR 2022, New Orleans, LA, USA, June 18-24, 2022*. IEEE, 11513–11522. <https://doi.org/10.1109/CVPR52688.2022.01123>
- [15] Xiaopeng Li, Bo Chen, Junda She, Shiteng Cao, You Wang, Qinlin Jia, Haiying He, Zheli Zhou, Zhao Liu, Ji Liu, et al. 2025. A Survey of Generative Recommendation from a Tri-Decoupled Perspective: Tokenization, Architecture, and Optimization. (2025).
- [16] Enze Liu, Bowen Zheng, Cheng Ling, Lantao Hu, Han Li, and Wayne Xin Zhao. 2025. Generative Recommender with End-to-End Learnable Item Tokenization. In *Proceedings of the 48th International ACM SIGIR Conference on Research and Development in Information Retrieval, SIGIR 2025, Padua, Italy, July 13-18, 2025*. ACM, 729–739. <https://doi.org/10.1145/3726302.3729989>
- [17] Enze Liu, Bowen Zheng, Wayne Xin Zhao, and Ji-Rong Wen. 2025. Bridging Textual-Collaborative Gap through Semantic Codes for Sequential Recommendation. In *Proceedings of the 31st ACM SIGKDD Conference on Knowledge Discovery and Data Mining, V2, KDD 2025, Toronto ON, Canada, August 3-7, 2025*. ACM, 1788–1798. <https://doi.org/10.1145/3711896.3736869>
- [18] Xinchun Luo, Jiangxia Cao, Tianyu Sun, Jinkai Yu, Rui Huang, Wei Yuan, Hezheng Lin, Yichen Zheng, Shiyao Wang, Qigen Hu, Changqing Qiu, Jiaqi Zhang, Xu Zhang, Zhiheng Yan, Jingming Zhang, Simin Zhang, Mingxing Wen, Zhaojie Liu, and Guorui Zhou. 2025. QARM: Quantitative Alignment Multi-Modal Recommendation at Kuaishou. In *Proceedings of the 34th ACM International Conference on Information and Knowledge Management, CIKM 2025, Seoul, Republic of Korea, November 10-14, 2025*. ACM, 5915–5922. <https://doi.org/10.1145/3746252.3761502>
- [19] Rayhane Mama, Marc S. Tyndel, Hashim Kadhim, Cole Clifford, and Ragavan Thuraiaratnam. 2021. NWT: Towards natural audio-to-video generation with representation learning. *CoRR* abs/2106.04283 (2021). arXiv:2106.04283 <https://arxiv.org/abs/2106.04283>
- [20] Fabian Mentzer, David Minnen, Eirikur Agustsson, and Michael Tschanen. 2024. Finite Scalar Quantization: VQ-VAE Made Simple. In *The Twelfth International Conference on Learning Representations, ICLR 2024, Vienna, Austria, May 7-11, 2024*. OpenReview.net. <https://openreview.net/forum?id=BishA3Ln8>
- [21] Jianmo Ni, Gustavo Hernández Ábrego, Noah Constant, Ji Ma, Keith B. Hall, Daniel Cer, and Yinfei Yang. 2022. Sentence-T5: Scalable Sentence Encoders from Pre-trained Text-to-Text Models. In *Findings of the Association for Computational Linguistics: ACL 2022, Dublin, Ireland, May 22-27, 2022*. Association for Computational Linguistics, 1864–1874. <https://doi.org/10.18653/V1/2022.FINDINGS-ACL.146>
- [22] Shashank Rajput, Nikhil Mehta, Anima Singh, Raghunandan Hulikal Keshavan, Trung Vu, Lukasz Heldt, Lichan Hong, Yi Tay, Vinh Q. Tran, Jonah Samost, Maciej Kula, Ed H. Chi, and Mahesh Sathiamoorthy. 2023. Recommendation Systems with Generative Retrieval. In *Advances in Neural Information Processing Systems 36: Annual Conference on Neural Information Processing Systems 2023, NeurIPS 2023, New Orleans, LA, USA, December 10 - 16, 2023*.
- [23] Anima Singh, Trung Vu, Nikhil Mehta, Raghunandan H. Keshavan, Maheswaran Sathiamoorthy, Yilin Zheng, Lichan Hong, Lukasz Heldt, Li Wei, Devansh Tandon, Ed H. Chi, and Xinyang Yi. 2024. Better Generalization with Semantic IDs: A Case Study in Ranking for Recommendations. In *Proceedings of the 18th ACM Conference on Recommender Systems, RecSys 2024, Bari, Italy, October 14-18, 2024*. ACM, 1039–1044. <https://doi.org/10.1145/3640457.3688190>
- [24] Aäron van den Oord, Oriol Vinyals, and Koray Kavukcuoglu. 2017. Neural Discrete Representation Learning. In *Advances in Neural Information Processing Systems 30: Annual Conference on Neural Information Processing Systems 2017, December 4-9, 2017, Long Beach, CA, USA*. 6306–6315.
- [25] Wenjie Wang, Honghui Bao, Xinyu Lin, Jizhi Zhang, Yongqi Li, Fuli Feng, Seekiong Ng, and Tat-Seng Chua. 2024. Learnable Item Tokenization for Generative Recommendation. In *Proceedings of the 33rd ACM International Conference on Information and Knowledge Management, CIKM 2024, Boise, ID, USA, October 21-25, 2024*. ACM, 2400–2409. <https://doi.org/10.1145/3627673.3679569>
- [26] Binrui Wu, Shisong Tang, Fan Li, Bing Han, Chang Meng, Jingyu Xiao, and Jiechao Gao. 2025. Aligning and Balancing ID and Multimodal Representations for Recommendation. In *Proceedings of the 31st ACM SIGKDD Conference on Knowledge Discovery and Data Mining, V2, KDD 2025, Toronto ON, Canada, August 3-7, 2025*. ACM, 5029–5038. <https://doi.org/10.1145/3711896.3737275>
- [27] Dongchao Yang, Songxiang Liu, Rongjie Huang, Jinchuan Tian, Chao Weng, and Yuexian Zou. 2023. HiFi-Codec: Group-residual Vector quantization for High Fidelity Audio Codec. *CoRR* abs/2305.02765 (2023). <https://doi.org/10.48550/ARXIV.2305.02765> arXiv:2305.02765
- [28] Xiaoyong Yang, Yadong Zhu, Yi Zhang, Xiaobo Wang, and Quan Yuan. 2020. Large Scale Product Graph Construction for Recommendation in E-commerce. *CoRR* abs/2010.05525 (2020). arXiv:2010.05525 <https://arxiv.org/abs/2010.05525>
- [29] Yining Yao, Ziwei Li, Shuwen Xiao, Boya Du, Jialin Zhu, Junjun Zheng, Xiangheng Kong, and Yuning Jiang. 2025. SaviorRec: Semantic-Behavior Alignment for Cold-Start Recommendation. *CoRR* abs/2508.01375 (2025). <https://doi.org/10.48550/ARXIV.2508.01375> arXiv:2508.01375
- [30] Wencai Ye, Mingjie Sun, Shaoyun Shi, Peng Wang, Wenjin Wu, and Peng Jiang. 2025. DAS: Dual-Aligned Semantic IDs Empowered Industrial Recommender System. In *Proceedings of the 34th ACM International Conference on Information and Knowledge Management, CIKM 2025, Seoul, Republic of Korea, November 10-14, 2025*. ACM, 6217–6224. <https://doi.org/10.1145/3746252.3761529>
- [31] Jiahui Yu, Xin Li, Jing Yu Koh, Han Zhang, Ruoming Pang, James Qin, Alexander Ku, Yuanzhong Xu, Jason Baldridge, and Yonghui Wu. 2022. Vector-quantized

- Image Modeling with Improved VQGAN. In *The Tenth International Conference on Learning Representations, ICLR 2022, Virtual Event, April 25-29, 2022*. OpenReview.net. <https://openreview.net/forum?id=pfNyExj7z2>
- [32] Neil Zeghidour, Alejandro Luebs, Ahmed Omran, Jan Skoglund, and Marco Tagliasacchi. 2022. SoundStream: An End-to-End Neural Audio Codec. *IEEE ACM Trans. Audio Speech Lang. Process.* 30 (2022), 495–507. <https://doi.org/10.1109/TASLP.2021.3129994>
- [33] Bowen Zheng, Yupeng Hou, Hongyu Lu, Yu Chen, Wayne Xin Zhao, Ming Chen, and Ji-Rong Wen. 2024. Adapting Large Language Models by Integrating Collaborative Semantics for Recommendation. In *40th IEEE International Conference on Data Engineering, ICDE 2024, Utrecht, The Netherlands, May 13-16, 2024*. IEEE, 1435–1448. <https://doi.org/10.1109/ICDE60146.2024.00118>
- [34] Carolina Zheng, Minhui Huang, Dmitrii Pedchenko, Kaushik Rangadurai, Siyu Wang, Fan Xia, Gaby Nahum, Jie Lei, Yang Yang, Tao Liu, Zutian Luo, Xiaohan Wei, Dinesh Ramasamy, Jiyan Han, Yiping Han, Lin Yang, Hangjun Xu, Rong Jin, and Shuang Yang. 2025. Enhancing Embedding Representation Stability in Recommendation Systems with Semantic ID. In *Proceedings of the Nineteenth ACM Conference on Recommender Systems, RecSys 2025, Prague, Czech Republic, September 22-26, 2025*. ACM, 954–957. <https://doi.org/10.1145/3705328.3748123>
- [35] Guorui Zhou, Jiaxin Deng, Jinghao Zhang, Kuo Cai, Lejian Ren, Qiang Luo, Qianqian Wang, Qigen Hu, Rui Huang, Shiyao Wang, Weifeng Ding, Wuchao Li, Xinchun Luo, Xingmei Wang, Zexuan Cheng, Zixing Zhang, Bin Zhang, Boxuan Wang, Chaoyi Ma, Chengru Song, Chenhui Wang, Di Wang, Dongxue Meng, Fan Yang, Fangyu Zhang, Feng Jiang, Fuxing Zhang, Gang Wang, Guowang Zhang, Han Li, Hengrui Hu, Hezheng Lin, Hongtao Cheng, Hongyang Cao, Huanjie Wang, Jiaming Huang, Jiapeng Chen, Jiaqiang Liu, Jinghui Jia, Kun Gai, Lantao Hu, Liang Zeng, Liao Yu, Qiang Wang, Qidong Zhou, Shengzhe Wang, Shihui He, Shuang Yang, Shujie Yang, Sui Huang, Tao Wu, Tiantian He, Tingting Gao, Wei Yuan, Xiao Liang, Xiaoxiao Xu, Xugang Liu, Yan Wang, Yi Wang, Yiwu Liu, Yue Song, Yufei Zhang, Yunfan Wu, Yunfeng Zhao, and Zhanyu Liu. 2025. OneRec Technical Report. *CoRR* abs/2506.13695 (2025). <https://doi.org/10.48550/ARXIV.2506.13695> arXiv:2506.13695
- [36] Guorui Zhou, Hengrui Hu, Hongtao Cheng, Huanjie Wang, Jiaxin Deng, Jinghao Zhang, Kuo Cai, Lejian Ren, Lu Ren, Liao Yu, Pengfei Zheng, Qiang Luo, Qianqian Wang, Qigen Hu, Rui Huang, Ruiming Tang, Shiyao Wang, Shujie Yang, Tao Wu, Wuchao Li, Xinchun Luo, Xingmei Wang, Yi Su, Yunfan Wu, Zexuan Cheng, Zhanyu Liu, Zixing Zhang, Bin Zhang, Boxuan Wang, Chaoyi Ma, Chengru Song, Chenhui Wang, Chenglong Chu, Di Wang, Dongxue Meng, Dunju Zang, Fan Yang, Fangyu Zhang, Feng Jiang, Fuxing Zhang, Gang Wang, Guowang Zhang, Han Li, Honghui Bao, Hongyang Cao, Jiaming Huang, Jiapeng Chen, Jiaqiang Liu, Jinghui Jia, Kun Gai, Lantao Hu, Liang Zeng, Qiang Wang, Qidong Zhou, Rongzhou Zhang, Shengzhe Wang, Shihui He, Shuang Yang, Siyang Mao, Sui Huang, Tiantian He, Tingting Gao, Wei Yuan, Xiao Liang, Xiaoxiao Xu, Xugang Liu, Yan Wang, Yang Zhou, Yi Wang, Yiwu Liu, Yue Song, Yufei Zhang, Yunfeng Zhao, Zhixin Ling, and Ziming Li. 2025. OneRec-V2 Technical Report. *CoRR* abs/2508.20900 (2025). <https://doi.org/10.48550/ARXIV.2508.20900> arXiv:2508.20900
- [37] Yongxin Zhu, Bocheng Li, Yifei Xin, Zhihua Xia, and Linli Xu. 2025. Addressing representation collapse in vector quantized models with one linear layer. In *Proceedings of the IEEE/CVF International Conference on Computer Vision, 22968–22977*.

## A Additional Experimental Details

### A.1 Baselines

We compare QuaSID with a set of strong vector-quantization-based baselines in our offline tokenizer evaluation. These methods differ in their quantization strategies, codebook optimization mechanisms, and gradient estimation techniques.

- **RQ-VAE** [14] recursively quantizes the residuals of dense item embeddings using multiple stacked codebooks, enabling a coarse-to-fine discretization. It is one of the most commonly adopted frameworks for semantic ID construction.
- **GRVQ** (Grouped Residual Vector Quantization) [27] partitions the embedding space into multiple groups and applies residual quantization independently within each group, aiming to reduce cross-dimension interference and improve codebook utilization.
- **Improved VQGAN** [31] adopts a low-dimensional codebook and applies  $\ell_2$ -normalized to both codebook vectors

and encoder outputs, effectively using cosine similarity for code assignment. This design encourages more uniform code utilization and improves reconstruction quality.

- **RQ-VAE-Rotation** [6] replaces the STE in RQ-VAE with the rotation trick, which leads to more informative gradients and improved quantization stability.
- **SimRQ** [37] freezes the codebooks and implicitly generates discrete codes via linear projections. This design mitigates codebook collapse and simplifies optimization, while preserving the hierarchical representation benefits of residual quantization.
- **RQ-OPQ** [2] combines residual quantization with optimized product quantization.
- **RQ-Kmeans** [18] is a two-stage semantic ID learning method that first aligns item representations based on item-item collaborative pairs, and then constructs residual quantization codebooks via a K-means-based mechanism to generate multi-layer discrete codes.

All methods use the same backbone model, and differ only in the tokenizer used to construct SIDs.

### A.2 Implementation Details

We use TIGER [22] as the generative recommendation backbone for all methods and keep identical model configurations across QuaSID and baselines. All offline experiments are implemented in PyTorch based on the open-source RQ-VAE recommender framework<sup>2</sup>. We optimize all generative models with Adam (lr  $3 \times 10^{-4}$ , weight decay  $1 \times 10^{-5}$ ) and batch size 256. Early stopping is applied if NDCG@5 + HitRate@5 does not improve for 10 consecutive validation checks. We adopt an 8-layer Transformer with 8 attention heads, embedding dimension 128, and MLP hidden dimension 512. All results are averaged over five random seeds.

For offline semantic ID learning, we use batch size 256 for all methods; for online A/B tests, we use batch size 1024. In offline public-dataset experiments, we set the number of codebook layers to  $L = 3$  and the codebook size to  $K = 256$  for a fair comparison across methods. In industrial experiments, we use  $L = 4$  and  $K = 1024$ . Baseline hyperparameters follow the original papers and are further tuned on validation sets. For QuaSID, we set the Hamming radius to  $R = 1$  for offline experiments and  $R = 2$  for online A/B tests, with margins  $m_{\text{full}} = 0.8$  and  $m_{\text{partial}} = 0.5$ . We tune  $\lambda_{cl} \in [0.01, 0.5]$ ,  $\lambda_{\text{full}} \in [0.05, 0.8]$ , and  $\lambda_{\text{partial}} \in [0.01, 0.8]$  on validation sets.

<sup>2</sup><https://github.com/EdoardoBotta/RQ-VAE-Recommender>